BULLETIN OF THE POLISH ACADEMY OF SCIENCES
TECHNICAL SCIENCES, Vol. 74(4), 2026, Article number: e158778
DOI: 10.24425/bpasts.2026.158778

The influence of compaction technology on the internal structure of the asphalt mixture

Marek IWAŃSKI* and **Małgorzata DURLEJ**

Kielce University of Technology, Faculty of Civil Engineering and Architecture, Al. Tysiąclecia P.P. 7, 25-314 Kielce, Poland

Abstract. A fundamental property of asphalt mixtures is the void content. It significantly influences their resistance to water and frost. Currently, this is traditionally determined using the hydrostatic method. This method may not be effective for environmentally friendly mixtures produced using Warm Mix Asphalt technology. They are produced and compacted at a lower temperature than traditional methods. Therefore, they may be characterized by abnormal void content in the internal structure. Microtomographic analysis can now be used to thoroughly examine the internal structure of asphalt mixtures in terms of pore size distribution, interconnection patterns, and their arrangement. This is particularly important in identifying changes occurring within the asphalt mixture as a result of the destructive effects of water and frost. Studies were conducted on the effect of vibratory and Marshall impact compaction on the internal structure of the asphalt mixture. Mixture samples were analyzed before and after conditioning according to AASHTO T283 and WT-2 2014 standards. It was found that the compaction method affects the distribution and interconnection of pores. Samples compacted using the vibratory method are more uniform in terms of the distribution of large and interconnected pores within the asphalt mixture structure. Smaller pores with a volume of 0 to 0.5 mm^3 occur between the mini-pores, increasing the resistance of the asphalt mixture to water and frost. It was found that, in addition to extremely small pores, interconnected pores have the greatest impact on the mixture resistance to water and frost.

Keywords: asphalt mixture; computed X-ray tomography; resistance to water and frost; internal structure.

1. INTRODUCTION

The implementation of sustainable management principles and environmentally friendly WMA (Warm Mix Asphalt) and HWMA (Half-Warm Mix Asphalt) technologies in road construction aligns with global sustainable development frameworks, such as the UN Sustainable Development Goals and the European Green Deal. However, the use of these types of asphalt mixtures requires special attention to analyzing their internal structure. This is because these types of asphalt mixtures, manufactured and laid at lower temperatures than traditional mixtures, may have an abnormal internal structure, potentially containing excessive voids. However, the internal structure of asphalt materials has a huge impact on their physical and mechanical properties, which determine their durability. It should be noted that one of the main characteristics of the durability of asphalt mixtures is their resistance to water and frost. This problem mainly concerns asphalt materials in the wearing course and is still very relevant, despite numerous studies in this area.

The loss of resistance of asphalt mixtures to the effects of water results in the washing out of asphalt from the aggregate surface, the detachment of aggregate grains, and the flaking and loosening the asphalt mixture. As a result, irregular cracks or deformations appear on the surface, which can cause complete degradation of the pavement. To ensure the resistance of the asphalt mixture to the destructive effects of water and frost, its compactness is assessed at the design stage and during the diagnosis of the road pavement structure. It should be noted that this parameter reflects the total content of free spaces without the possibility to analyze the number of pores, their size, and the way they are connected in the internal structure. Therefore, it is not possible to predict how the size and quantity of pores will change during the exploitation of the pavement and, consequently, the durability of the pavement over its long service life. Thus, it is extremely challenging to predict the resistance of asphalt mixtures to the effects of water and frost [1, 2]. This problem becomes even more serious, as indicated by Chomicz-Kowalska *et al.* [3,4], in the case of WMA and HWMA mixtures produced and laid at low temperatures, which may affect their compaction [5]. Moreover, it should be noted that the correct compaction and the properties of asphalt mixtures are also influenced by material factors such as the type of asphalt, modifiers, the type of aggregate, and its mineralogical composition, which affect the adhesion of asphalt to the aggregate, as demonstrated in the studies by Mazurek and Iwański [6] and Mielczarek *et al.* [7]. The properties of the asphalt mixture produced, and the technology used in its production also have a significant impact on its resistance to water and frost. This relationship has been proven, among others, in studies. Mixtures with an air void content ranging from 8% to 10% are most vulnerable to water [8], which is called the 'worst pore' effect. Less 'sensitive' are mixtures containing more than 12% free space, in which water can freely flow out of the mixture. The least sensitive are those with a free space content of less than 3–5%. However, the amount of free space does not determine whether water will get

*e-mail: iwanski@tu.kielce.pl

Manuscript submitted 2025-11-02, revised 2026-03-14, initially accepted for publication 2026-04-13, published in July 2026.

under the surface or not. Studies have shown that mixtures with similar air void content can vary significantly in terms of permeability. This is primarily due to the composition of the mineral mixture, namely the use of different types of aggregates and different contents of their individual fractions, as shown in the study by Nogueria [9]. Permeability is determined by the internal structure of the mixture, not just the content of free spaces. Therefore, permeability testing, characterized by the number and type of pores in the internal structure, can better determine the sensitivity of a given mixture to water and frost than the free space content only. For this purpose, the X-ray CT tomography method can be used, which has been in use in medicine since 1973. However, the first diagnostic studies of the microstructure of asphalt mixtures were conducted at the end of the last century. In recent years, interest in the use of microcomputed tomography (microCT) in the testing of building materials has grown significantly due to the desire to ensure their greater durability. The studies focused on assessing the internal structure in terms of the content and spatial distribution of asphalt, aggregate grains, and the density of free spaces [10]. Masad *et al.* [11] made a significant contribution to the development of X-ray CT in the diagnosis of asphalt mixtures. This method was used to compare the internal structure of asphalt concrete samples compacted using a vibratory press and a plate compactor. The tests showed that the distribution of grains in samples compacted using the second method is much more random and haphazard. A similar analysis was carried out by Masad *et al.* [11] on samples compacted at different speeds on a vibratory press and on cores taken from the field. They found that the anisotropy in the vibratory samples becomes more pronounced to a certain extent as the compaction force increases. A further increase in force results in a reduction in anisotropy and a more random grain orientation. A similar relationship was demonstrated by Saadeh *et al.* and Tashman *et al.* [12, 13]. Based on microCT analyses, Alvarez *et al.* [14, 15] noted the need to modify the process of preparing vibratory press samples to reduce the significant vertical and horizontal heterogeneity present in their internal structure, i.e., the vertical and horizontal distribution of the total void content, their volume, and interconnected voids. Muray's research demonstrated a significant effect of compaction on the internal structure of asphalt mixtures [16]. Ji *et al.* demonstrated that in samples of WMA asphalt mixtures with the addition of synthetic wax, the distribution of voids is related to grain size and the compaction method [17]. Furthermore, the presence and distribution of voids in AC mixtures significantly affect their basic properties, especially resistance to water and frost, as demonstrated by studies by Alawneh *et al.* [18] and Iwański and Durlej [19]. However, it is still important to identify changes in the internal structure of asphalt mixtures exposed to water and frost, as well as the impact of compaction methods on them. Identifying the changes occurring in the structure of asphalt mixtures may contribute to the development of requirements ensuring their long-term durability during exploitation.

The study aimed to determine the impact of the internal structure of the asphalt mixture on its resistance to water and frost, depending on the compaction and conditioning method. The study compared the results of computer microtomography analysis of asphalt concrete samples conditioned using two methods – AASHTO T283 [20] and the procedure described in Appendix 1 to WT-2 2014 [21]. The AASHTO T283 procedure is characterized by a more aggressive impact of water and frost on the asphalt mixture than the WT-2 2014 procedure. The asphalt mixture was compacted using a vibratory and impact compactor to assess the effectiveness of these compaction processes on the formation of the internal structure of the asphalt mixture. The method of compacting asphalt mixture using a vibratory and impact compactor was applied to assess the effectiveness of these compaction processes on the formation of the internal structure of the asphalt mixture. Their internal structure was compared before and after conditioning, and an analysis of its change and the manner of their connection was performed. Based on the results obtained, the impact of compaction and conditioning methods on the internal structure was assessed. The results obtained will be significant in the implementation of the X-ray CT tomography procedure for the diagnosis of mixtures produced using WMA and HWMA technology. This is crucial for ensuring their required operational durability. These types of mineral-asphalt mixtures are compacted at a temperature of approximately 125–130°C, which is approximately 35°C lower than traditional mineral-asphalt mixtures. Consequently, they may be undercompacted, which will result in an abnormal internal structure – the structure and distribution of pores. Consequently, they may not meet the water and frost resistance criteria.

2. MATERIALS AND METHODS

The analyzed mixture was asphalt concrete intended for the wearing course. Polymer-modified asphalt 45/80-55 was used as a binder. The mineral mixture used limestone and gabbro aggregate. The ingredients and proportions of the mineral mixture are listed in Table 1. This mixture was marked as AC 11S and made in HMA technology at a temperature of 165°C. To improve the adhesion of the asphalt to the aggregate, a surfactant additive of 0.3% was used. The mixture was previously tested

Table 1
The composition of the mineral mix and the asphalt content in the investigated AC 11S asphalt concrete

Materials	Mineral mixture (% w/w)	Asphalt mix (% w/w)
Filler (limestone aggregate)	4.0	3.8
Crushed fine, continuously graded aggregate 0/2 mm (limestone)	19.0	18.0
Coarse aggregate 0/4 mm (limestone)	18.0	17.0
Coarse aggregate 2/5 mm (gabbro)	18.0	17.0
Coarse aggregate 4/8 mm (gabbro)	13.0	12.3
Coarse aggregate 8/11.2 mm (gabbro)	28.0	26.5
45/80-55 penetration paving grade bitumen	–	5.4
Total	100.0	100.0

in terms of fulfilling the technical requirements described in WT-2 2014 – part I [21]. The required properties of the AC 11S mixture are listed in Table 2. Four sets of samples of the same mixture were prepared to perform tomography tests, with each set consisting of seven samples. Two sets were compacted using the impact method, and two using a gyratory compactor. The samples were prepared according to the EN 12697-30 [22] and EN 12697-31 standards [23], so they were cylinders with a diameter of 100 mm and a height of about 63.5 mm. The samples were formed at 145°C. Compaction with an impact compactor involved 35 blows per side. Forming the samples using a gyratory compactor involved 40 rotations.

Table 2
Properties of asphalt concrete AC 11S

Property	Testing method	Required value	The obtained average value
Air void content V_a [%]	EN 12697-8	V_{min} – 2.0 V_{max} – 4.0	$V_{ŚR}$ – 2.9
Resistance to permanent deformation: WTS_{AIR} [mm/10^3 cycles], PRD_{AIR} [%]	EN 12697-22 (procedure B)	PRD_{AIR} – 9.0 WTS_{AIR} – 0.15	PRD_{AIR} – 8.2 WTS_{AIR} – 0.06
Resistance to water and frost ITSR [%]	EN 12697-12, WT-2 2014	ITSR – 90	ITSR – 91

The prepared mixture samples were conditioned according to the procedures described in AASHTO T283 and to WT2-2014. Four different combinations were obtained: 1 – impact-compacted samples conditioned according to AASHTO T283, 2 – impact-compacted samples subjected to ITSR testing, 3 – samples made using a gyratory compactor, conditioned according to AASHTO T283, and 4 – samples made using a gyratory compactor, subjected to ITSR testing. Asphalt mixture samples should be saturated with water to a moisture content of 70–80%, according to the methodology presented in [20,21]. The method described in WT-2 2014 involves conditioning the soaked samples at 40°C for 68–72 hours, then freezing them for at least 16 hours at −18°C. The samples are then placed in a water bath at 25°C for 24 hours. The AASHTO T283 method, however, requires that after soaking the samples in water, they be frozen at −18°C for at least 16 hours and then placed in a water bath at 60°C for 24 hours. After the conditioning process, the samples were kept in a dry, air-dried state at a temperature of 25°C for 24 hours. The samples were then scanned.

The main part of the testing was to scan the samples before and after conditioning. CT (Computed Tomography) is a type of X-ray spectroscopy – a diagnostic method that allows obtaining layered images of the examined object. It uses a composite of object projections made from different directions to create cross-sectional (2D) and spatial (3D) images.

Creating a tomographic image involves measuring the absorption of radiation passing through an object, as demonstrated in detail by Zapała-Sławeta [24] during tests on the alkaline reactivity of aggregates.

The volume of the object is divided into small cells, called voxels, in which the linear radiation absorption coefficient is the same. The distribution of radiation absorption coefficients is calculated by a computer, which is why the method is called computed tomography. The basic method of testing is to direct an X-ray beam at the tested object and record its intensity on the other side on a detector panel. One property of this type of radiation is that it can travel through matter, losing energy along the way, according to Beer's law.

The scan is done by X-ray irradiating the object during rotation of the sample through 360° in relation to the stationary lamp and detector (Fig. 1), as detailed in the studies by Liu *et al.* [25]. The accuracy of the final mapping depends on the number of projections performed during the rotation of the object. Having projection images for multiple element sections, the image of the entire element is reconstructed by the Radon transform. This allows for the reconstruction of a three-dimensional image of the object from multiple projections of the element, as demonstrated by Alvarez *et al.* [26] in their study of the effect of rubber on the structure of asphalt mixtures.

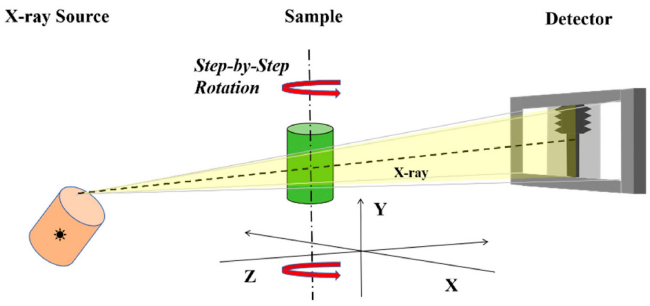

Fig. 1. Schematic of the X-ray CT system [26]

The practical result is a three-dimensional grayscale image in which each shade of gray corresponds to a specific density value. Lighter tones represent higher densities, while darker ones indicate materials of lower density.

The structure of the samples was assessed in a Nikon XT H 225 ST computed tomography machine. A rotating target generating a conical beam was used in the research. Its maximum voltage is 225 kV, and the power is 450 W. The scans were done by using a voltage of 223 kV and a current of 512 μA. Additionally, a 2 mm thick copper filter was used. The values were selected experimentally to obtain the best scanning parameters for the type of analyzed samples. The three-dimensional model of the object was created from the assembly of 4477 images with a resolution of approx. 45 μm for each of the samples. It was obtained by data reconstruction and its initial processing – noise reduction, edge sharpening, and the use of filters in the CT Pro 3D program.

For structural analysis, three samples with the most similar pore content were selected from each set. Before computational analysis, the samples were trimmed to the same volume in the program to eliminate pores and irregularities on their surface. The same sample part/volume was analyzed before and after conditioning. Determination of the air void content with the use of microCT was based on the use of the 'porosity/inclusions

analysis' tool available in Volume Graphics Studio Max 2023.1. The total pore content in each volume was calculated for each sample. An analysis of the directional variability of the free space content along the height of the sample was performed. The percentage of free spaces in different zones of the sample was compared. Additionally, the analysis obtained the size distribution of air voids, i.e., their diameters and volumes. A 3D model of free spaces was created for each sample. A visual analysis of possible cracks formed after conditioning of the samples was performed.

3. RESULTS AND DISCUSSION

The method of compacting asphalt mixture samples may affect the arrangement of grains and the arrangement and distribution of air voids. Also, the pore connections and permeability of the samples may be determined by the forming method used. Therefore, 2D cross-sections of the samples were generated to detect possible differences. Each set of samples was subjected to quantitative analysis, which allowed for the determination of the average percentage of free spaces, both before and after the freezing process. The results are summarized in Table 3. Additionally, to illustrate the location and connections of free spaces, a 3D model of air voids was generated for each sample – both before and after conditioning. Selected sets of 3D models (before and after freezing) for each of the four combinations are shown in Figs. 2–5.

Table 3
Average air void content in samples before and after conditioning

Compaction method	Impact				Rotational			
Conditioning method	WT-2 2014 Annex 1		AASHTO T283		WT-2 2014 Annex 1		AASHTO T283	
	$\overline{V}_a$	σ %	$\overline{V}_a$	σ %	$\overline{V}_a$	σ %	$\overline{V}_a$	σ %
Average air void content before conditioning [%]	2.42	0.46	2.33	0.21	2.41	0.11	2.77	0.16
Average air void content after conditioning [%]	2.58	0.48	2.75	0.29	2.52	0.12	3.12	0.11
Difference	0.16	0.12	0.42	0.09	0.11	0.08	0.35	0.24
Percentage difference [%]	6.56	2.13	18.06	2.60	4.71	2.53	12.73	3.11

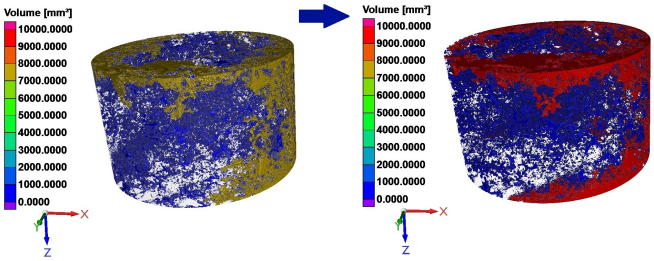

Fig. 2. Example of 3D models of air voids of the HMA AC 11 S mixture impact compacted and conditioned according to Annex 1 WT-2 2014

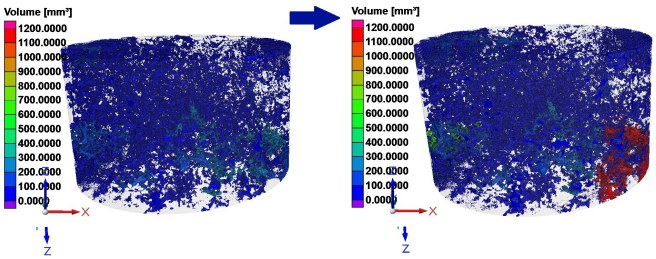

Fig. 3. Example of 3D models of air voids of the HMA AC 11 S mixture impact compacted and conditioned according to AASHTO T283

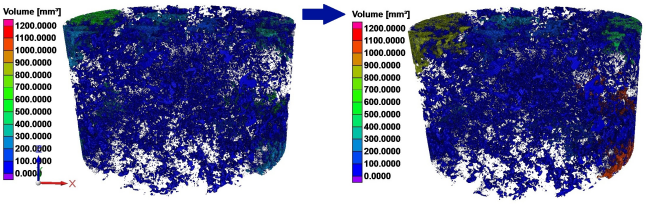

Fig. 4. Example of 3D models of air voids of the HMA AC 11 S mixture rotationally compacted and conditioned according to Annex 1 WT-2 2014

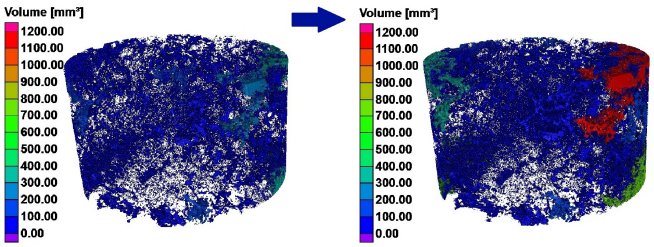

Fig. 5. Example of 3D models of air voids of the HMA AC 11 S mixture rotationally compacted and conditioned according to AASHTO T283

The visual analysis of cross-sections and 3D models shows that samples compacted using the impact method in the extreme parts (outer, upper, and lower) are characterized by lower compaction compared to those formed rotationally. For this reason, the air voids within these parts are more connected, which may be the reason for higher permeability. The volume of the connected voids reaches up to 7000–8000 mm^3. Better connection of air voids and, therefore, higher permeability in the outer parts of the samples may be the reason for greater changes occurring in impact-compacted samples as a result of their conditioning.

This is confirmed by the results presented in Table 3. The change in the average void content is more noticeable in impact-compacted samples. It should also be noted that conditioning of the samples using the AASHTO T283 method resulted in more visible changes in the internal structure. This tendency occurs for both compaction methods.

Additionally, quantitative analysis was performed to prove slightly more uniform compaction in samples made using the

Table 4
Average percentage of air voids in the external and internal parts of the samples

Compaction method	Conditioning method	Average air void content before conditioning [%]				Average air void content after conditioning [%]				Difference between parts before conditioning		Difference between parts after conditioning	
Part		Inner part		Outer part		Inner part		Outer part					
		$\overline{V}_a$	σ (%)	$\overline{V}_a$	σ (%)	$\overline{V}_a$	σ (%)	$\overline{V}_a$	σ (%)	$\overline{V}_a$	σ (%)	$\overline{V}_a$	σ (%)
Impact	WT-2 2014, annex no. 1	1.24	0.10	3.56	0.85	1.45	0.03	4.06	1.12	2.32	0.81	2.61	1.09
	AASHTO T283	1.18	0.09	3.48	0.79	1.33	0.04	4.18	1.24	2.29	0.83	2.86	1.12
Rotational	WT-2 2014, annex no. 1	1.56	0.14	3.23	0.11	1.63	0.12	3.38	0.13	1.66	0.13	1.75	0.07
	AASHTO T283	1.93	0.15	3.59	0.19	2.08	0,08	4.14	0.17	1.66	0.12	2.06	0.15

gyratory press. Table 4 shows the average percentage of free spaces in the external and internal parts samples from each set. The samples were divided in such a way that the volumes of individual parts were similar. The method of division in the cross-section and 3D model is shown in Fig. 6.

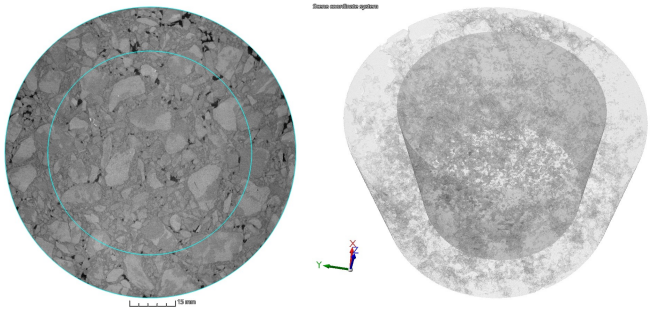

Fig. 6. Method of dividing samples to analyze their homogeneity – on the left, 2D cross-section, on the right, 3D model

As shown in Table 4, the differences between the internal and external parts of the samples are lower for those compacted using the rotational method, ~ 1.66%. For the impact method, the difference is ~ 2.3%. It can also be noticed that the impact-formed samples have a denser (~ 1.2%) internal part compared to the second method. It can therefore be assumed that in impact-compacted samples, there will be more closed pores inside the sample, and its external part will be more permeable. Additionally, sample conditioning intensifies the differences in the content of air voids between zones, and this is much more visible for impact-compacted samples. Furthermore, the presented results regarding changes in the conditioning context support the previously mentioned conclusions that the AASHTO T283 method is slightly more destructive. Perhaps the reason is the occurrence of greater thermal shock.

It is assumed that the compaction method affects differences in the arrangement of aggregate grains, and therefore also the arrangement and size of air voids. To verify the impact of this arrangement on air voids, further analysis compared the distribution of the volume of air voids. For each set of samples, charts were made of the quantitative distribution of air voids according to their volume in the range of 0–10 mm^3 before and after conditioning (Fig. 7). Pores in this range constitute 98–99% of all air voids in quantitative terms, regardless of the compaction method.

It is assumed that the compaction method affects differences in the arrangement of aggregate grains, and therefore also the arrangement and size of air voids. To verify the impact of this arrangement on air voids, further analysis compared the distribution of the volume of air voids. For each set of samples, charts were made of the quantitative distribution of air voids according to their volume in the range of 0–10 mm^3 before and after conditioning (Fig. 7). Pores in this range constitute 98–99% of all air voids in quantitative terms, regardless of the compaction method.

The graphs presented in Fig. 7 show that in the case of both sample forming methods, the largest volume compartment is 0–0.5 mm^3, about a million occurrences. Conditioning does not affect major changes in this area. This compartment is still the largest after conditioning. The second largest interval is 0.5–1 mm^3. However, in the case of the rotational method, it is slightly less numerous. In subsequent intervals, as the pore volume increases, their number decreases. A slightly stronger decrease is visible in rotationally compacted samples. Changes in compartments caused by conditioning do not show a specific trend. Based on these graphs, it is not possible to clearly determine which samples (either impact or rotationally compacted) featured greater changes and which conditioning method had a greater impact on the microstructure.

To clarify the results, pores from the largest range (0–0.5 mm^3) were subjected to a more detailed analysis. Pie charts were made of the percentage share of narrower ranges of air void volumes in the total pore volume from the range of 0–0.5 mm^3. Pie charts of the percentage of individual volume intervals of free spaces in the range of 0–0.5 mm^3 before and after conditioning of the samples are shown in Figs. 8–11. The standard deviation of the test results across the various pore size ranges was between 0.15 and 0.53%.

The analysis of pie charts for samples compacted with a Marshall tamper shows that the largest share is recorded by pores with volumes of 0–0.05 mm^3. Similarly to the column chart, you can see the relationship: the larger the pore volume, the smaller their share. In the case of these two sets, it is noticeable

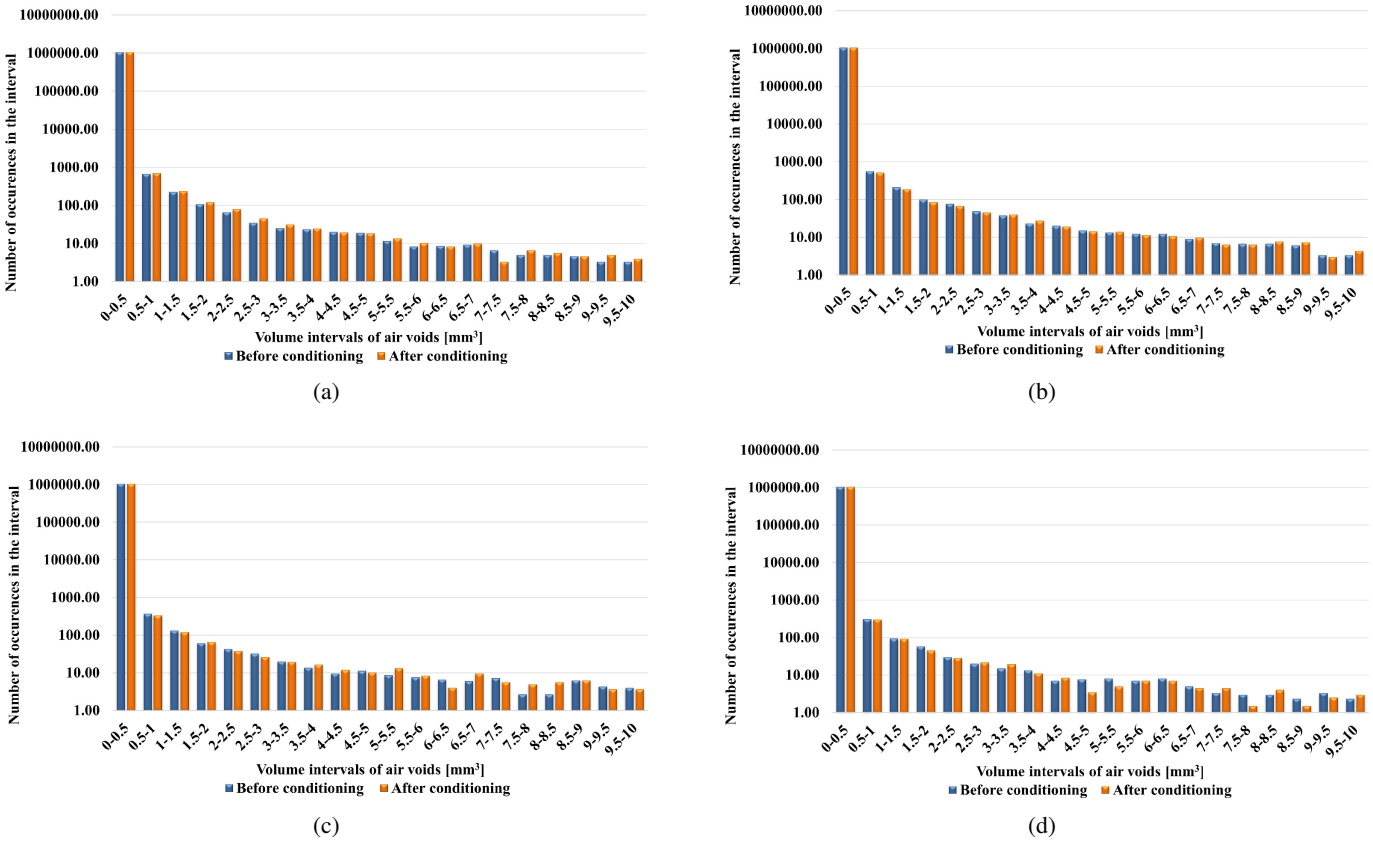

Fig. 7. Quantitative distribution of air voids according to their volume in the range 0–10 mm^3: (a) impact compacted, WT-2 2014 conditioned; (b) impact compacted, AASHTO T283 conditioned; (c) rotational compacted, WT-2 2014 conditioned; (d) rotational compacted, AASHTO T283 conditioned

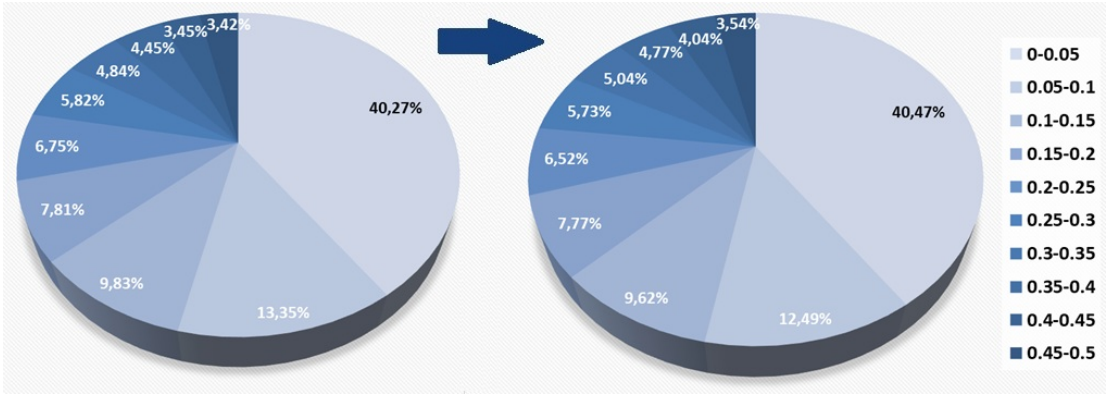

Fig. 8. Percentage of individual volume intervals of free spaces in impact-compacted samples in the range of 0–0.5 mm^3 before and after conditioning of samples according to Annex 1 WT-2 2014

that conditioning causes an increase in the share of the smallest pores. However, this type of change is more intense as a result of sample conditioning according to AASHTO T283. The change in this case is over 5%.

Based on the graphs, it can be seen that sets of samples formed using a gyrator compactor contain a higher proportion of the smallest air voids compared to those compacted using an impact method. Here, their share exceeds 50%. Interestingly, the share of the previously mentioned group of pores in the set conditioned according to WT-2 2014 decreases, while after conditioning according to AASHTO T283 it increases. The value of these changes also varies. The decrease is almost 5%, while the increase is approximately 2%. The decrease in the content of pores with a volume of 0–0.05 mm^3 is the effect of their joining as a result of washing away by water and bursting during freezing. This is confirmed by the increase in the share of the next volume groups, especially 0.05–0.1 mm^3. The reason for the apparent differences in microstructure changes with respect to

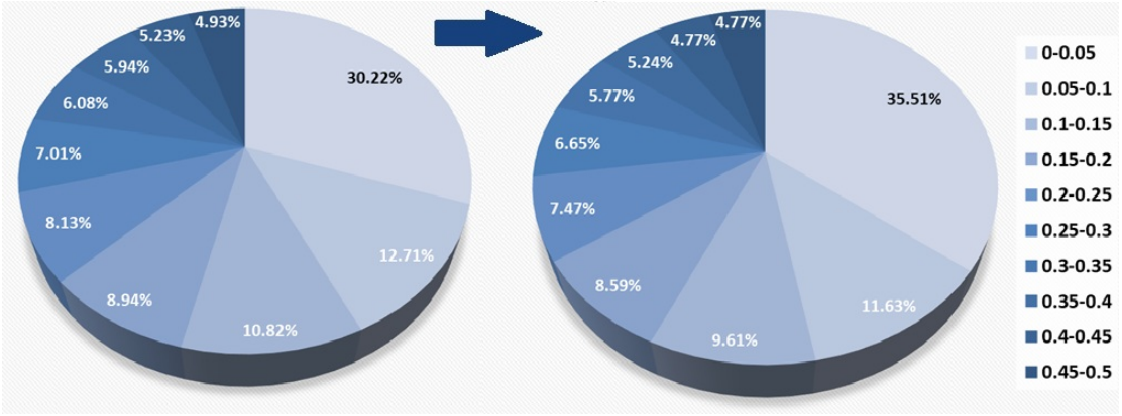

Fig. 9. Percentage of individual volume intervals of free spaces in impact-compacted samples in the range of 0–0.5 mm^3 before and after conditioning of samples according to AASHTO T283

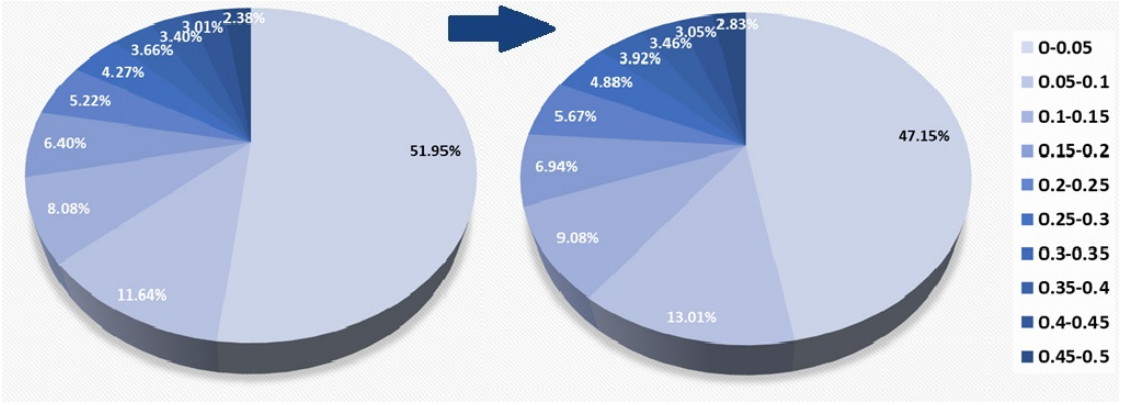

Fig. 10. Percentage of individual volume intervals of free spaces in rotational-compacted samples in the range of 0–0.5 mm^3 before and after conditioning of samples according to Annex 1 WT-2 2014

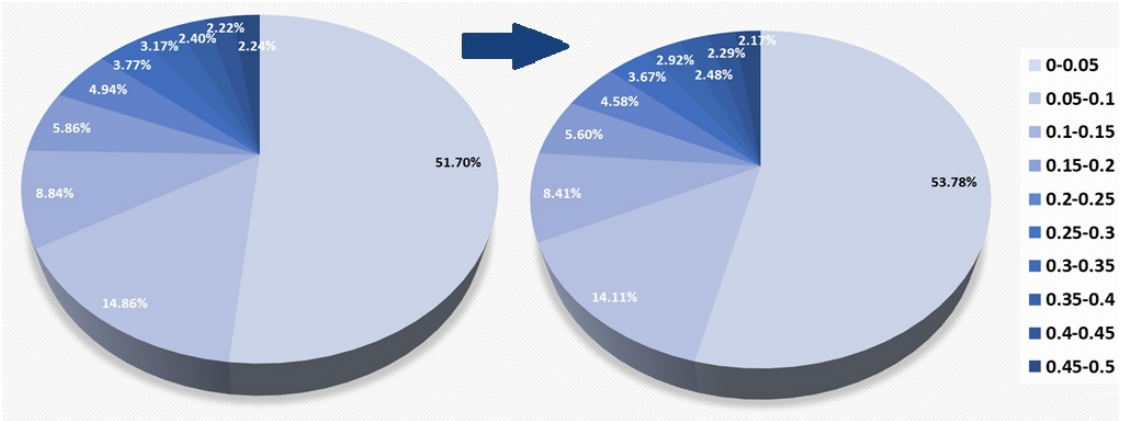

Fig. 11. Percentage of individual volume intervals of free spaces in rotational-compacted samples in the range of 0–0.5 mm^3 before and after conditioning of samples according to AASHTO T283

different conditioning methods may be the more destructive effect of the AASHTO T283 method. It is possible that this method causes greater removal of asphalt due to the higher storage temperature in the bath (60°C). As a result, smaller voids merge, but new ones are also created to compensate for their percentage share. The results presented for impact-compacted samples confirm this thesis. The increase in the share of the volume group 0–0.05 mm^3 after conditioning according to WT-2 2014 is minimal, 0.2%. However, the increase after AASHTO T283 is about 5%, similar to samples from the gyrator compactor. This minimal increase may be due to the greater susceptibility of samples compacted with a Marshall t amper to water and frost.

4. CONCLUSIONS

Based on research and analyses conducted, the following conclusions were formulated:

- The method of compacting samples affects the arrangement and connections of the air voids contained in them. The outer parts of asphalt concrete samples compacted with a Marshall tamper are more permeable and therefore more susceptible to water and frost.
- Samples compacted using a gyratory press are more homogeneous, with a difference between the outer and inner parts being only 1.66%. For impact-compacted samples, it is approximately 2.3%. In vibratory compacted samples, air voids are less connected (their volume before conditioning is a maximum of 500 mm^3), which makes the samples slightly less susceptible to water and frost.
- The AASHTO T283 method causes greater changes in the internal structure of asphalt concrete than conditioning, according to Annex 1 to WT-2 2014.
- The most numerous group of pores is that with a volume of 0 to 0.5 mm^3, i.e., about a million pores. Within this group, there are visible changes caused by the impact of water and frost. Apart from extremely small pores, connected pores have the greatest impact on the susceptibility of asphalt concrete to water and frost.

These studies have a significant impact on the development of a new, advanced methodology for testing the resistance of asphalt mixtures to water and frost, particularly in relation to WMA and HWMA mixtures. This methodology will enable the optimization of compaction temperatures while ensuring the required long-term durability of asphalt pavements.

ACKNOWLEDGEMENTS

The research work was funded by the Kielce University of Technology of Poland, grant number 02.0.09.00/1.02.001.SUBB.BKIK.26.002.

REFERENCES

[1] S.G. Jahromi, "Estimation of resistance to moisture destruction in asphalt mixtures," *Constr. Build. Mater.*, vol. 23, pp. 2324–2331, 2009, doi: 10.1016/j.conbuildmat.2008.11.007.

[2] P. Jaskula and J. Judycki, "Verification of the criteria for evaluation of water and frost resistance of asphalt concrete," *Road Mater. Pavement Des.*, vol. 9, no. 1, pp. 135–162, 2008, doi: 10.1080/14680629.2008.9690163.

[3] A. Chomicz-Kowalska, W. Gardziejczyk, and M.M. Iwański, "Moisture resistance and compatibility of asphalt concrete produced in half-warm mix asphalt technology with foamed bitumen," *Constr. Build. Mater.*, vol. 126, 124214, pp. 108–118, 2016, doi: 10.1016/j.conbuildmat.2021.124214.

[4] A. Chomicz-Kowalska, K. Maciejewski, M.M. Iwański, and K. Janus, "Effects of zeolites and hydrated lime on volumetrics and moisture resistance of foamed warm mix asphalt concrete," *Bull. Pol. Acad. Sci. Tech. Sci.*, vol. 69, no. 2, pp. e136731, 2021, doi: 10.24425/bpasts.2021.136731.

[5] J. Mrugala and M.M. Iwański, "Resistance to permanent deformation of asphalt concrete with F-T wax modified foamed bitumen," *Procedia Eng.*, vol. 108, pp. 459–466, 2015, doi: 10.1016/j.proeng.2015.06.171.

[6] G. Mazurek and M. Iwański, "Analysis of selected properties of asphalt concrete with synthetic wax," *Bull. Pol. Acad. Sci. Tech. Sci.*, vol. 66, no. 2, pp. 2017–228, 2018, doi: 10.24425/122102.

[7] M. Mielczarek, K. Andrzejczak, and M. Słowik, "Three-factor assessment of rutting factor of modified asphalt binders and mastics in the ageing process," *Bull. Pol. Acad. Sci. Tech. Sci.*, vol. 73, no. 3, pp. 373–381, 2025, e153833, doi: 10.24425/bpasts.2025.15383.

[8] E. Masad, B. Muhunthan, N. Shashidhar, and T. Harman, "Internal structure characterization of asphalt concrete using image analysis," *J. Comput. Civ. Eng.*, vol. 13, no. 2, pp. 88–95, 1999, doi: 10.1061/(ASCE)0887-3801.

[9] P. Nogueira, "Characterization of the air void content of fine aggregate matrices within asphalt concrete mixtures," *Constr. Build. Mater.*, vol. 300, p. 124214, 2021, doi: 10.1016/j.conbuildmat.2021.124214.

[10] K. Gopalakrishnan, H. Ceylan and F. Inanc, "Using x-ray computed tomography to study paving materials," *Proc. Inst. Civ. Eng., Constr. Mater.*, vol. 160, no. 1, 2007, pp. 15–23, doi: 10.1680/coma.2007.160.1.15.

[11] E. Masad, B. Muhunthan, N. Shashidhar, and T. Harman, "Quantifying laboratory compaction effects on the internal structure of asphalt concrete," *Transp. Res. Rec.*, vol. 1681, no. 1, pp. 179–185, 1999, doi: 10.3141/1681-21.

[12] S. Saadeh, L. Tashman, E. Masad, and W. Mogawer, "Spatial and directional distributions of aggregates in asphalt mixes," *J. Test. Eval.*, vol. 30, no. 6, pp. 483–491, 2002, doi: 10.1520/JTE12345J.

[13] L. Tashman, E. Masad, B. Peterson, and H. Saleh, "Internal structure analysis of asphalt mixes to improve the simulation of superpave gyratory compaction to field conditions," *Association of Asphalt Paving Technologists-Proc. Technical Sessions. Asphalt Paving Technology* 2001, Clearwater Beach, US, 19–21 Mar. 2001, vol. 70, pp. 605–64.

[14] A.E. Alvarez, A. Epps Martin, and C. Estakhri, "Internal structure of compacted permeable friction course mixes," *Constr. Build. Mater.*, vol. 24, no. 6, pp. 1027–1035, 2010, doi: 10.1016/j.conbuildmat.2009.11.015.

[15] A.E. Alvarez, J.S. Carvajal, O.J. Reyes, C. Estakhri, and L.F. Walubita, "Image analysis of the internal structure of warm mix asphalt (wma) mixtures," *Proc. TRB 91st Annual Meeting*, 2012, pp. 1–17.

[16] P.M. Muraya, "Homogeneous test specimens from gyratory compaction," *Int. J. Pavement Eng.*, vol. 8, no. 3, pp. 225–235, 2007, doi: 10.1080/10298430701289323.

[17] J. Ji, Z. Yuan, Z. Suo, Y. Xu, P. Li and Z. You, "Moisture susceptibility of warm mix asphalt (WMA) with an organic wax additive based on X-ray computed tomography (CT) technology." *Adv. Civ. Eng.*, vol. 2019, p. 7101982, 2019, doi: 10.1155/2019/7101982.

[18] M. Alawneh, H. Soliman and A. Anthony, "Characterizing the Effect of Freeze–Thaw Cycling on Pore Structure of Asphalt Concrete Mixtures Using X-ray CT Scanning," *Materials*, vol. 16, p. 6254, 2023, doi: 10.3390/ma16186254.

[19] M.M. Iwański and M. Durlej, "Diagnostyka mieszanki mineralno-asfaltowej na etapie badań laboratoryjnych z wykorzystaniem

tomografu materiałowego," (Diagnostics of the asphalt mixture at the stage of laboratory tests using a material tomograph – in Polish). *Inżynieria i Budownictwo*, vol. 6, pp. 413–417, 2024, doi: 10.5604/01.3001.0054.7479.

[20] AASHTO T283-22, Resistance of Compacted Asphalt Mixtures to Moisture-Induced Damage, 2022.

[21] WT-2, Technical Guidelines 2, Asphalt Pavements for National Roads. Part I: Asphalt Mixes. General Directorate for National Roads and Motorways, Warsaw, 2014.

[22] EN 12697-30:2019, Bituminous mixtures – Test methods – Part 30: Preparation of compacted samples.

[23] EN 12697-31:2019, Bituminous mixtures – Test methods – Part 31: Specimen preparation by gyratory compactor.

[24] J. Zapała-Sławeta, "The use of computed tomography and scanning miscroscopy methods for assessing the alkaline reactivity of aggregate," *Bull. Pol. Acad. Sci. Tech. Sci.*, vol. 72, no. 3, p. e149814, 2024, doi: 10.24425/bpasts.2024.149814.

[25] Z. Liu, Z. Liu, Y. Huang and Y. Cao, "Determining the Compaction Temperature of Warm-Mix Anti-Rutting Asphalt Mixture," *Appl. Sci.*, vol. 14, p. 11042, 2024, doi: 10.3390/app142311042.

[26] A.E. Alvarez, E.M. Fernandez, A. Epps Martin, O.J. Reyes, G.S. Simate and L.F. Walubita, "Comparison of permeable friction course mixtures fabricated using asphalt rubber and performance-grade asphalt binders," *Constr. Build. Mater.*, vol. 28, pp. 427–436, 2012. doi: 10.1016/j.conbuildmat.2011.08.085.